Leukemia Research 108 (2021) 106626

Contents lists available at ScienceDirect

Leukemia Research

journal homepage: www.elsevier.com/locate/leukres

An antibody-drug conjugate with intracellular drug release properties showing specific cytotoxicity against CD7-positive cells

Jing Zhang [a,1], Arvind Jain [a,2], Sabine Milhas [a,3], Daniel J. Williamson [b], Justyna Mysliwy [b], Adam Lodge [b], Jenny Thirlway [b], Majid Al Nakeeb [b], Ami Miller [a,c], Terry H. Rabbitts [a,c,*]

[a] Weatherall Institute of Molecular Medicine, MRC Molecular Haematology Unit, University of Oxford, Oxford, OX3 9DS, UK
[b] Iksuda Therapeutics, The Biosphere, Draymans Way, Newcastle Helix, Newcastle upon Tyne, NE4 5BX, UK
[c] Institute of Cancer Research, Division of Cancer Therapeutics, 15 Cotswold Road, Sutton, London, SM2 5NG, UK

ARTICLE INFO

Keywords:
Leukaemia
CD7
ADC
Antibody
T cell leukaemia
Intracellular drug delivery

ABSTRACT

Refractory T cell acute leukaemias that no longer respond to treatment would benefit from new modalities that target T cell-specific surface proteins. T cell associated surface proteins (the surfaceome) offer possible therapy targets to reduce tumour burden but also target the leukaemia-initiating cells from which tumours recur. Recent studies of the T cell leukaemia surfaceome confirmed that CD7 is highly expressed in overt disease. We have used an anti-CD7 antibody drug conjugate (ADC) to show that the binding of antibody to surface CD7 protein results in rapid internalization of the antigen together with the ADC. As a consequence, cell killing was observed *via* induction of apoptosis and was dependent on cell surface CD7. The *in vitro* cytotoxic activity (EC_{50}) of the anti-CD7 ADC on T cell acute leukaemia (T-ALL) cells Jurkat and KOPT-K1 was found to be in the range of 5−8 ng/mL. In a pre-clinical xenograft model of human tumour growth expressing CD7 antigen, growth was curtailed by a single dose of ADC. The data indicate that CD7 targeting ADCs may be developed into an important second stage therapy for T cell acute leukaemia, for refractory CD7-positive leukaemias and for subsets of acute myeloid leukaemia (AML) expressing CD7.

1. Introduction

T-cell acute lymphoblastic leukaemia (T-ALL) is an aggressive malignancy that occurs in all age groups. It represents 10 %–15 % of pediatric ALLs and 20 % of adult ALLs [1,2]. T-ALL in children and younger adults is usually treated with high dose of chemotherapy resulting in survival rates of approximately 80 %. Adult patients suffer a much lower 5-year overall survival rate of around 50 %. Further, relapsed T-ALL is particularly difficult to salvage with 20 % for paediatric and less than 7 % for adult patients surviving at 5 years [3,4], implying that chemo-resistant minimal residual disease persists as leukaemia initiating cells (LICs) after primary treatment and propagates relapsed disease. Cancer therapy has been revolutionized in the past few years both in oncology and hematology because of recent developments in immunotherapy. In addition to providing novel therapeutic agents, immunotherapy could help reduce the side effects often associated with conventional chemotherapeutic treatments, which are usually non-specific and affect normal cells. However, novel therapeutic choices are limited. An anti-CD52 antibody, alemtuzumab [5], currently in development, has only demonstrated modest activity and causes significant side effects.

T-ALL is commonly associated with chromosomal translocations and rearrangements including *LMO1, LMO2, HOX11/TLX1, TAL1/SCL, TAL2, LYL1* and *BHLHB1* [6–13], resulting in their aberrant expression in developing thymocytes and blocked differentiation of T-cell progenitors [14]. The lymphoblasts in T-ALL have variable expression of CD1a, CD2, CD3, CD4, CD5, CD7 and CD8. CD7 is a transmembrane glycoprotein that starts to appear in the early stages of T cell differentiation from stem cells and expression persists to the mature T-cells. Although also expressed on normal T cells, CD7 is absent in a subset of normal CD4-positive T cells [15]. CD7 is thought to be involved in T-cell and T-cell/B-cell interactions during early lymphoid development and

* Corresponding author at: Weatherall Institute of Molecular Medicine, MRC Molecular Haematology Unit, University of Oxford, Oxford, OX3 9DS, UK.
E-mail addresses: jing.zhang3@ucb.com (J. Zhang), terry.rabbitts@icr.ac.uk (T.H. Rabbitts).
[1] Jing Zhang: UCB Pharma, 216 Bath Road, Slough, SL1 3WE, UK.
[2] Arvind Jain: Sun Pharma Advanced Research Company Ltd., Sun Pharma Road, Tandalja, Vadodara- 390012, India.
[3] Sabine Milhas: Vertex Pharmaceuticals, 88 Jubilee Avenue, Milton Park, OX14 4RW, UK.

https://doi.org/10.1016/j.leukres.2021.106626
Received 27 March 2021; Received in revised form 11 May 2021; Accepted 14 May 2021
Available online 18 May 2021

has been recognized as a co-stimulatory molecule with CD3, CD45, PI3K [16–18]. Investigations into T-cell leukaemia-initiating cells (T-LICs) suggested that CD7 is highly expressed on almost all T-ALL patient samples together with other LIC-associated cell surface markers including CD53, CD59a and GPR56 [19]. In addition, the CD34 and CD7 double positive cells also demonstrated leukaemia initiating activity in contrast to the CD34+/CD7− sub-population. [20]. In addition to T-ALL, CD7 is also expressed in about 30 % of AML cells [21,22].

A series of studies focused on conjugating immunotoxins to anti-CD7 antibodies in various forms, including a mouse monoclonal antibody [23], single-chain Fv [24] or nanobody [25], have been carried out aiming to treat T cell malignancies. Despite the potent effect on CD7 positive cells both *in vitro* and *in vivo*, none of these immunotoxins have been approved for clinical use. A phase I clinical trial of an anti-CD7-ricin A-chain showed two partial responses and one minimal response in five patients receiving maximally tolerated dose (MTD). However, vascular leak syndrome (VLS) occurred as a dose-limiting toxicity (DLT) [26], potentially due to the ricin A-chain immunotoxin, which damages human endothelial cells [27]. Therefore, new therapeutic agents with enhanced safety and potency profiles would be beneficial for treating T-ALL. Antibody-drug conjugates (ADCs) are one option and have been the focus of intense interest as a means to provide selective tumour killing with increased efficacy and fewer side effects than standard of care chemotherapies. ADCs comprise a monoclonal antibody (or antibody fragment) that targets a tumour-associated antigen, conjugated *via* a chemical linker to a highly cytotoxic entity. Binding of the antibody to the cell surface triggers internalization, and processing within endosomes or lysosomes releases the potent cell killing molecule. Combining the targeting power of an antibody with a potent cytotoxic agent makes it possible to eradicate cancer cells more effectively and selectively, while reducing the side effects which undermine patient quality of life. Monomethyl auristatin E (MMAE) is a highly-toxic anti-mitotic agent that blocks the polymerization of tubulin, resulting in suppression of tumour cell viability. MMAE cannot be used as a drug *per se* due to its high toxicity, however, ADCs employing MMAE have been shown to be highly effective [28]. MMAE has been tested with various antibodies resulting in three FDA approved ADCs, Brentuximab vedotin (anti-CD30), polatuzumab vedotin (anti-CD79b), enfortumab vedotin (anti-Nectin-4) and several other ADCs in different stages of development [29].

ADCs require efficient internalization and a stable linker for drug conjugation that is cleavable only in cells. We have conjugated MMAE to a chimaeric anti-human CD7 bivalent antibody using the highly stable PermaLink® bioconjugation chemistry [30] and an intracellular cleavable peptide spacer. We demonstrate that this anti-CD7-ADC shows specific and potent cytotoxic activity against CD7-expressing cells both *in vitro* and *in vivo*. With further development, this CD7 targeting ADC could be an effective treatment for CD7-expressing cancers.

2. Material and methods

2.1. Cells and tissue culture

Jurkat, KOPT-K1 cells and human PBMC cells were cultured in RPMI1640 medium supplemented with 10 % FBS (Sigma F7524) and Penicillin Streptomycin (Gibco 15140-122). A549, A549-CD7 and SKBR3 cells were cultured in DMEM (Gibco 31966-021) medium supplemented with 10 % FBS and Penicillin Streptomycin.

2.2. Generation of stable cell line A549-CD7

The pcDNA3.1-ZEO CD7 vector (gift from Dr. Linda Baum) was linearized at the BglII restriction site and transfected into a total of 5×10^6 A549 cells using lipofectamine 2000. Cells were sorted into 96-well plates at 1 cell per well using flow cytometry. Stable clones were selected with 100 μg/mL of zeocin (Gibco R25001). The expression of CD7 was confirmed by anti-CD7 antibody and flow cytometry (Supplementary Fig. S2 and Supplementary Table S1).

2.3. Antibody production

The variable regions of anti-CD7 from pET26b anti-CD7 scFv cys vector (gift from Georg Fey) were amplified using PCR and cloned into VH-expression vector VHExpress, which incorporates the human Cγ1 gene and Vκ-expression vector VKExpress, which carries human Cκ gene [31]. The sequence of the final anti-CD7 IgG is shown in Supplementary Fig. S5. The expression vectors were linearized by EcoRI digestion and transfected into NS0 cells using Neon Transfection System (Thermo Fisher Scientific) according to the manufacture's protocol. A total of 2×10^6 NS0 cells were resuspended with 0.1 mL of buffer R and transfected with a mixture of 500 ng of linearized anti-CD7-VH vector and 50 ng of linearized anti-CD7-Vκ vector at the setting of 1350 V, 20 ms, 2 pulses. Stable cell lines were selected with 0.4 mg/mL G418 and tested for IgG antibody expression by immunoblotting using goat anti-human IgG (H + L) HRP-coupled secondary antibody (Invitrogen 31410). An IgG-producing clone NS0_anti-CD7_6 was used for antibody production by culturing in CD Hybridoma Medium (Gibco 11279023) supplemented with 8 mM of GlutaMAX (Gibco 35050038), cholesterol lipid (Gibco 12531018) and Penicillin Streptomycin (Gibco 15140-122) for 7 days in roller bottles. The supernatant was collected, cleared by centrifugation (30 min, 4000 *g*) followed by passing through a 0.22 μm filter. The antibody-containing supernatant was applied to a HiTrap Protein G HP column (GE Healthcare 17040501) and purified using AKTA (GE Healthcare). The antibody was eluted with 0.1 M glycine-HCl (pH 2.7). The eluate was immediately neutralized with 1 M Tris−HCl (pH 9.0), concentrated and then buffer exchanged to PBS pH 7.4 (Gilbco 10010-015) using Amicon centrifugal filter units (EMD Millipore UFC901008). The purified antibody was reduced with 5 % of 2-Mercaptoethanol (Sigma-Aldrich M3148) and analysed using 12 % SDS-PAGE.

2.4. Labeling of the anti-CD7 IgG with Alexa Fluor 488

The purified anti-CD7 (human IgG) antibody was buffer exchanged to 0.1 M sodium bicarbonate buffer pH 8.3, and concentrated to 10 mg/mL using Amicon centrifugal filter units. 1 mg of the antibody was conjugated with 0.1 mg of Amine-reactive dye Alexa Fluor 488 5-SDP Ester (Life Technologies A30052) at room temperature for 1 h. The excess dye was removed by dialysis against PBS pH 7.4. The Alexa Fluor 488 labelled antibody was concentrated using Amicon centrifugal filter units.

2.5. Live cell image of the anti-CD7 internalization

The RPMI1640 medium containing 10 % (vol/vol) fetal bovine serum was cooled to 4 °C prior to the experiment. Jurkat cells were prepared at 5×10^5 cells/mL in the cold medium. The Alexa Fluor 488-labeled anti-CD7 antibody was added to the cell suspension at the final concentration of 10 μg/mL and incubated on ice for 30 min followed by washing and resuspending cells at 2×10^5 cells/mL in ice-cold medium. The antibody-bound-cells were transferred to a μ-slide 8 well chamber (ibidi 80821) and incubated at 37 °C and 5 % CO_2 for live cell imaging. Images were collected at 5 s intervals for 20 min using a DeltaVision Elite Imaging System.

2.6. Generation of antibody-PermaLink-MMAE conjugates

Purified anti-CD7 antibody was reduced and conjugated to PermaLink-PEG4-Val-Cit-PAB-MMAE using the conditions described in Supplementary Table S2. The conjugate (0.92 mg/mL, 6.2 μM) was isolated from the excess linker-toxin and organic solvent into PBS using desalting columns following manufacturer's instructions. The sample was analyzed by HPLC using polymer-linked reverse-phase (PLRP) to

establish the drug-antibody ratio (DAR) of the ADC. The ADC and antibody protein concentrations were determined using UV spectroscopy and the A_{280} nm extinction coefficients 213320 M^{-1} cm^{-1} or 1.42 (A0.1 %).

Herceptin (Roche) was reduced and conjugated to PermaLink-PEG4-Val-Cit-PAB-MMAE using the conditions described in Supplementary Table S4. The ADC (1.81 mg/mL, 12.4 μM) was isolated from the excess linker-toxin and organic solvent into PBS using desalting columns following manufacturer's instructions. The sample was analyzed by HPLC using PLRP to establish the DAR of the ADC.

2.7. Internalization assay

Jurkat, KOPT-K1 or MOLT4 cells were seeded in 75 cm^2 cell culture flasks at 2×10^5 cells/mL and incubated at 37 °C, 5 % CO_2 overnight. A total of 2×10^6 cells was resuspended in 200 μL of PBS with 10 % FBS in a centrifuge tube and incubated with 1 μg of purified anti-CD7 antibody on ice for 30 min. The cell suspension was split into two aliquots of 10^6 cells: one aliquot was kept on ice and one was incubated at 37 °C for 90 min. Both aliquots of cells were washed once with 5 mL ice-cold PBS + 10 % FBS and collected by centrifuging for 5 min at 4 °C, 200×*g*. Cells were fixed with 4 % formaldehyde at room temperature for 15 min and transferred onto coverslips with a Cytospin. Cells were permeabilized with 0.5 % Tween in PBS for 15 min and blocked with blocking buffer (PBS with 10 % FBS and 0.1 % Tween) for 30 min at room temperature. The endosomal marker EEA1 or lysosomal marker LAMP1 were labelled with primary antibodies (Cell Signaling, 1:200 dilution) for 1 h. Cells were then incubated with a mixture of anti-rabbit secondary antibody and anti-human secondary antibody (Invitrogen, 1:200 dilution) for another 1 h. Coverslips were washed 3 times with PBS and then mounted with DAP-containing Fluoromount-G (SouthernBiotech 0100-01) overnight. Slides were analyzed using a Zeiss 880 inverted LSM confocal microscope with a 63x objective. Primary antibodies: EEA1 Rabbit mAb: Cell Signaling 3288S, LAMP1 Rabbit mAb: Cell Signaling 9091S. Secondary antibody: Alexa Fluor 594 donkey anti-rabbit IgG (H + L) antibody: Invitrogen A-21207, Alexa Fluor 488 goat anti-human IgG (H + L) antibody: Invitrogen A-11013. The number of surface-CD7 molecules on each type of cells, determined by the antibody binding capacity, was estimated using BD Quantibrite Beads (Supplementary Table S1).

2.8. Viability assays

Cell viability was measured using the CellTiter-Glo luminescent cell viability assay (Promega G7573). Cells were cultured at 5×10^4 cells/mL in 100 μL of growth medium in 96-well plates and incubated for 72 h. For viability assay, 100 μL of CellTiter-Glo reagent was added to each well and mixed by gentle shaking. The plate was incubated at room temperature for 10 min and the luminescence recorded using a plate reader (PerkinElmer, 2103 Envision).

2.9. Cell apoptosis assay

Cells were plated at 5×10^4/mL and treated with 1 μg/mL of anti-CD7 or 1 μg/mL of anti-CD7-MMAE or 5 μM of etoposide for 24 h at 37 °C. Following the treatment, cells were counted to have 5×10^4 cells per staining reaction. Each cell aliquot was washed in 3 mL of buffer (10 mM HEPES, pH 7.4, 140 mM NaCl, 2.5 mM $CaCl_2$), pelleted at 200 × g for 5 min at 4 °C and resuspended in 100 μL of buffer containing 5 μL of FITC Annexin-V (BD 556420). Cells were stained with Annexin V on ice for 15 min before washing with 3 mL of buffer. Finally, cells were resuspended in 0.5 mL of fresh buffer containing 0.25 μg of 7-AAD (BD 559925), incubated on ice for another 10 min and processed to flow cytometric analysis without washing using Attune NxT flow cytometer (ThermoFisher).

2.10. In vivo experiments

Mouse xenografts were carried out by Axis Bioservices. A total of 25 male athymic nude mice aged 5−8 weeks and weighing approximately 27−35 g were used for the study. Animals were housed in IVC cages (up to 5 per cage) with individual mice identified by tail mark. All animals were allowed free access to a standard certified commercial diet and sanitised water during the study. All protocols used in this study were approved by the Axis Bioservices Animal Welfare and Ethical Review Committee, and all procedures were carried out under the guidelines of the Animal (Scientific Procedures) Act 1986. A total of5×10^6 A549-CD7 cells (1:1 with Matrigel) were implanted onto the flank of male athymic nude nu/nu mice using a 23-gauge needle. Once tumours reached 100−150 mm^3 the mice were randomly assigned to treatment groups (Fig. 5A) and received a single dose of drug as indicated. Tumours were measured 3 times per week and were allowed to grow for up to 36 days.

3. Results

3.1. Internalization of anti-CD7 antibody

Recombinant anti-human CD7 antibody was produced from NS0 stable cells in a chemically defined medium. The VH and VL chains from an anti-CD7 single chain Fv (a gift from Dr. Georg Fey) were cloned into a human IgG1 expression plasmid system [31] and stably transfected into NS0 cells as described in Methods. The antibody was purified from the cell culture using a protein G column and analyzed on 12 % SDS-PAGE (Supplementary Fig. S1A). The specific binding of the purified antibody was confirmed using CD7-expressing T cell lines (Jurkat, MOLT4 and KOPT-K1) and a lung cancer cell line (A549) that was stably transfected to express CD7 (A549-CD7), compared with CD7-negative cells (A549, or the breast cancer cell line SKBR3) (Supplementary Fig. S2). The binding of control ADC, anti-Her2-MMAE, to these cells was also analyzed (Supplementary Fig. S2). The relative numbers of CD7 molecules on the surface of the T cell lines compared to A549-CD7 were estimated by flow cytometry (Supplementary Table S1).

The ability of CD7-anti-CD7 interaction to cause internalization was analyzed using confocal microscopy and time lapse videos. As shown in Fig. 1, binding of anti-CD7 to Jurkat (Fig. 1A), KOPT-K1 cells (Fig. 1B) and to human peripheral blood mononuclear cells (Fig. 1C, PBMC) resulted in internalization of the antibody and co-localization with the endosome/lysosome compartments within 90 min when incubated at 37 °C. Essentially no CD7 internalization was observed at the same time when the cells were incubated at 4 °C. The internalization of the surface CD7, following binding to the bivalent anti-CD7 antibody, occurs by capping and internalization of the surface-bound antibody shown using live-cell imagining (Supplementary video S1).

3.2. Generation and characterization of anti-CD7 antibody drug conjugates

The anti-CD7-MMAE ADC (Supplementary Fig. S1B) was generated by conjugating MMAE molecules to the cysteine residues in the hinge region of the anti-CD7 antibody *via* PermaLink® bioconjugation chemistry and a cathepsin B cleavable peptide linker, which facilitates the release of the MMAE inside the endosome/lysosome upon internalization of the ADC into the target cell [32] (Supplementary Fig. S1C). The anti-CD7 IgG was successively reduced and conjugated to PermaLink-PEG4-Val-Cit-PAB-MMAE using the conditions described in Supplementary Table S2. The conjugate was isolated from the excess linker-toxin and organic solvent into PBS using desalting columns. The sample was analyzed by HPLC using polymer-linked reverse-phase (PLRP) to establish the drug-antibody ratio (DAR) of the ADC (Supplementary Table S3). The DAR was estimated to be 2.6 by PLRP (Supplementary Fig. S3). The consequence of conjugation on antigen binding

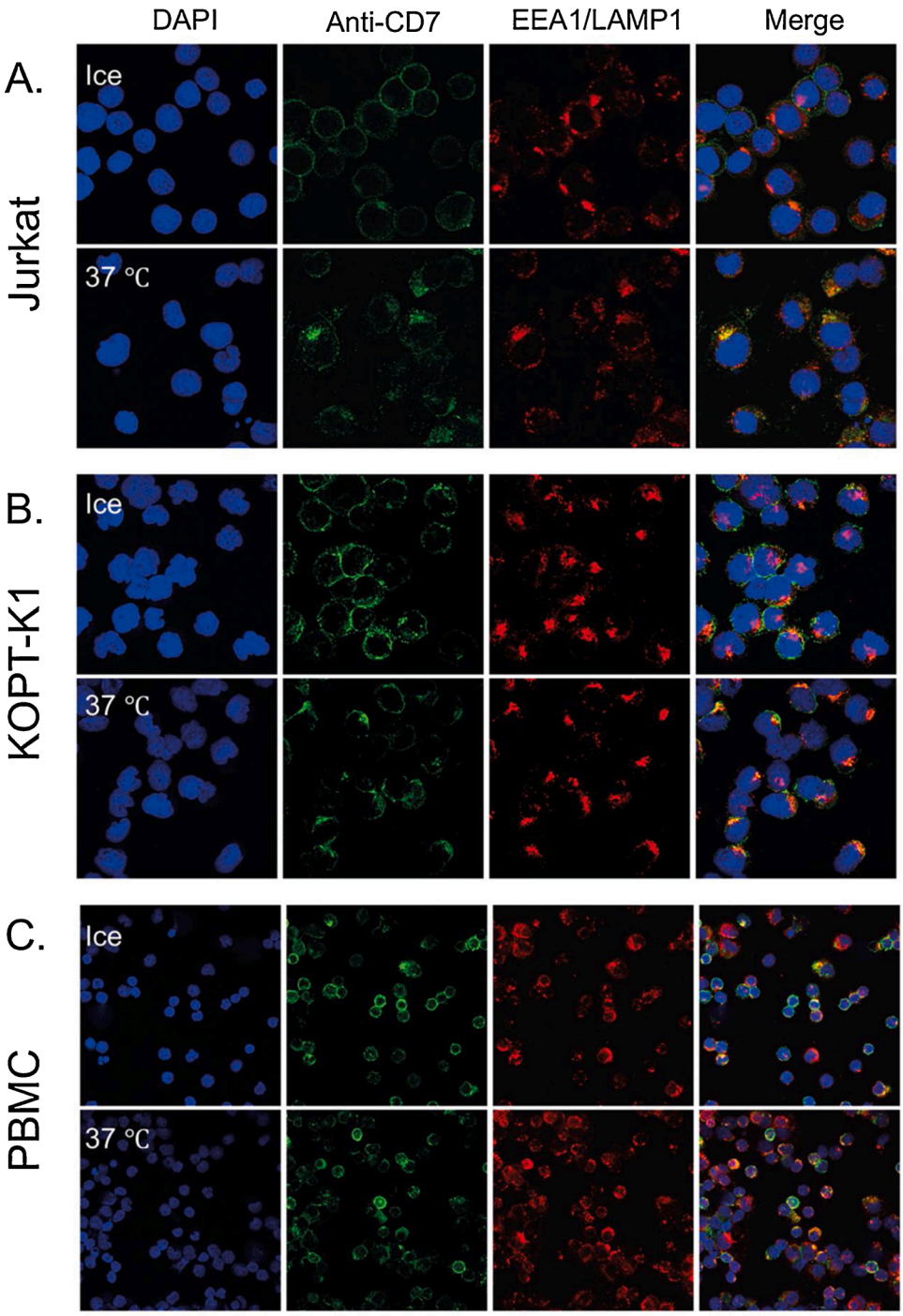

Fig. 1. Internalization of anti-CD7 antibody by T cells and human PBMC.
T cell lines Jurkat (A), KOPT-K1 (B) and human PBMC (C) were incubated with anti-CD7 chimeric antibody for 1.5 h at 4 °C or 37 °C. Cells were fixed and incubated with a mixture of rabbit monoclonal antibodies binding to the endosomal marker EEA1 and the lysosomal marker LAMP1. The bound antibodies were detected by incubation with Alexa Fluor 488-labeled (green) secondary anti-human antibody (detecting anti-CD7) or Alexa Fluor 594-labeled (red) secondary anti-rabbit antibody (detecting anti-EEA1 and anti-LAMP1). Cell nuclei were stained using DAPI (blue). The merged images (right hand panels) show co-localization of internalized anti-CD7 antibody and endosome/lysosome proteins (yellow).

was evaluated by binding either anti-CD7-MMAE or unconjugated anti-CD7 antibody to Jurkat, MOLT-4 and KOPT-K1 cells, which endogenously express CD7 (Supplementary Fig. S2). Both anti-CD7 antibody and anti-CD7-MMAE bound specifically to the CD7 positive cells.

3.3. *Cytotoxicity of CD7+ cells caused by anti-CD7-MMAE ADC in vitro*

The cytotoxicity of anti-CD7-MMAE was assessed *in vitro* in the A549-CD7 cell line and was highly active (Fig. 2A) but showed no activity on the parental A549 cells that lack human CD7 expression (Fig. 2B). This further demonstrates that the cytotoxic effect was dependent on specific binding through the antibody component of the conjugate. In addition, the anti-CD7 antibody alone did not show cytotoxicity in either cell line. (Fig. 2A, B). The effect of anti-CD7-MMAE was compared to anti-Her2-MMAE ADC in the two human T-ALL cell lines expressing surface CD7 (Jurkat and KOPT-K1) and a breast cancer cell line (SKBR3) that is epidermal growth factor receptor 2 (HER2)-positive and CD7 negative. The anti-CD7-MMAE has an IC_{50} of 5.4 ng/mL and 8.1 ng/mL on Jurkat or KOPT-K1 cells respectively (Fig. 2C, D), but is not active on SKBR-3 breast cancer cells (Fig. 2E). By contrast, SKBR3 cells are killed by the anti-Her2-MMAE (IC_{50} is 4.8 ng/mL). The anti-Her2 ADC completely kills SKBR3 while CD7 ADC only reaches 80–90 % loss of viability in the T cells as well as in the A549-CD7 lung cell line. This could be due to relative sensitivities of the different cell lines to MMAE. There is no correlation between IC_{50} and level of CD7 expression on cells like A549-

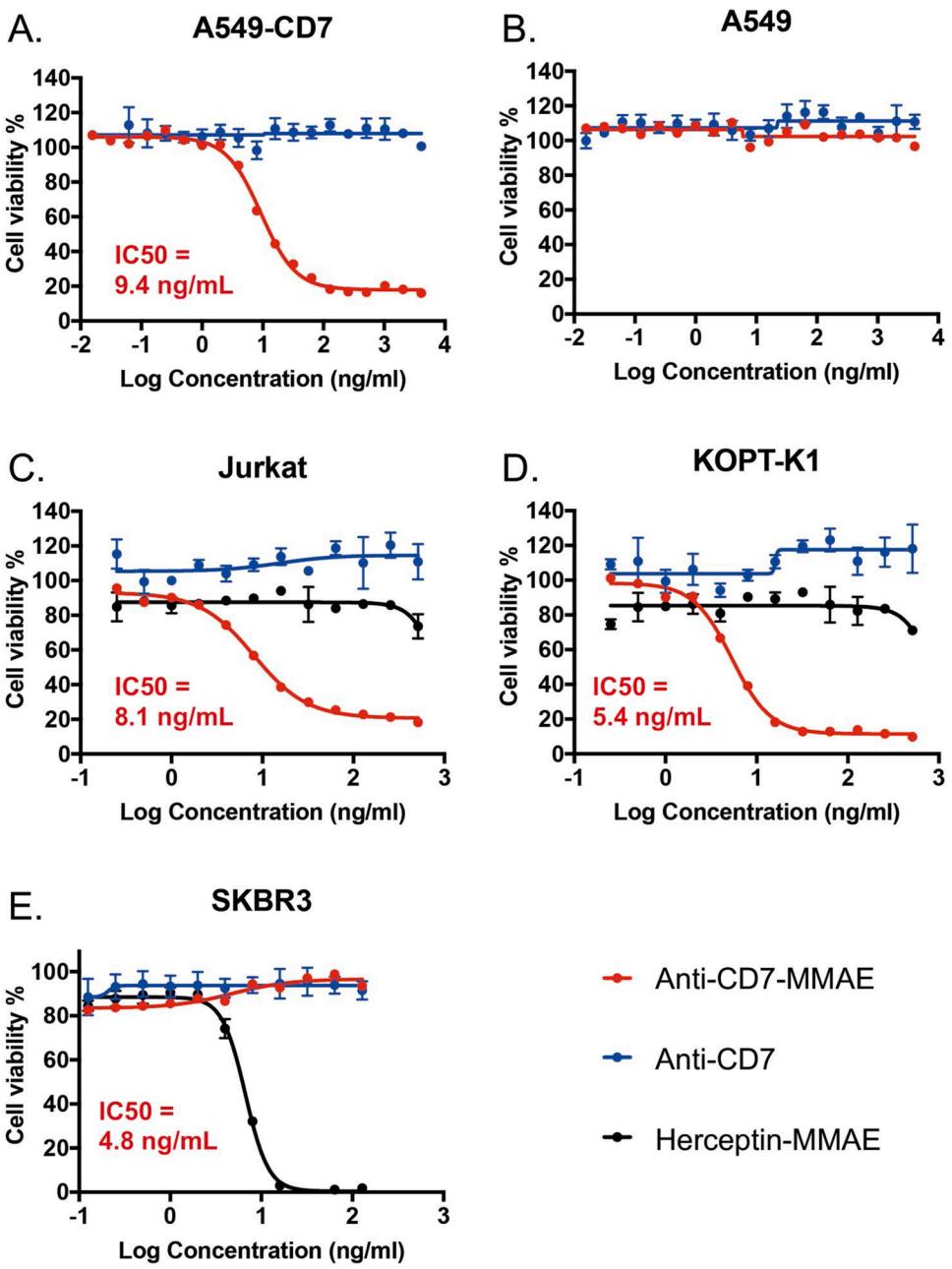

Fig. 2. Anti-CD7 ADC is cytotoxic to cells expressing CD7.
Anti-CD7-MMAE ADC or anti-CD7 IgG were incubated with A549 cells expressing human CD7 (panel A), A549 cells (panel B), Jurkat T cells (panel C), KOPT-KI T cells (panel D), with increasing doses as shown on the x axis. In addition, the T cell lines (C and D) were incubated with anti-Her2-MMAE. The breast cancer cell line SKBR3 (E) was incubated with all three antibodies/ADCs. The cell viabilities were measured using CellTitreGlo assays and the data are shown as mean values ± standard deviation of 3 or more samples. IC_{50} values were determined using curve fitting by nonlinear regression as the concentration of the drug that causes 50 % loss of cell viability compared to untreated cells.

CD7 (with 144,000 molecules of CD7, Supplementary Table S1) that show $IC_{50} = 9.4$ ng/mL in comparison to Jurkat cells with $IC_{50} = 8.2$ ng/mL (with 7960 CD7 molecules per cell, Supplementary Table S1). The similar potency of anti-CD7-PermaLink-MMAE on cells with lower and higher target expression shows that there is a threshold expression level of CD7 required to deliver enough MMAE to induce cell death.

We analyzed the mechanism of cell cytotoxicity *via* an Annexin V and 7-amino-actinomycin D (7-AAD) binding assay. FITC-labeled Annexin V was used to identify apoptotic cells by binding to phosphatidylserine, which is translocated to the external leaflet of the plasma membrane during cell apoptosis. The 7-AAD discriminates between intact and dead cells by staining the DNA of the dead cells. More than 50 % of Jurkat cells or KOPT-K1 cells undergo apoptosis (Fig. 3A, B) suggesting the anti-CD7 ADC induces programmed cell death.

3.4. Localization and internalization of anti-CD7 ADC in vivo

The cell-based assays demonstrate that the anti-CD7-ADC is a potent, specific cytotoxic reagent for CD7-expressing cells (Fig. 2). We examined the properties of systemically delivered ADC in a transgenic mouse strain (hCD7 Tg mice) that expresses human CD7 in leucocytes, particularly in the spleen [33]. hCD7 mice were injected with anti-CD7 antibody or anti-CD7-MMAE or PBS and sacrificed 48 h after injection. Splenocytes were prepared and stained with FITC-labelled anti-human Ig antibody (to detect injected chimaeric anti-CD7 antibody or ADC) and FITC-labelled anti-CD7 antibody to detect transgenic CD7 expression. The anti-human Ig secondary antibody was observed to bind splenocytes from the mice injected with anti-CD7 antibody or anti-CD7-MMAE, but not with PBS, indicating the injected antibody or ADC was localized to the CD7 on the splenocytes and continued to be replaced by fresh circulating antibody as it becomes internalized. This was supported by our finding that FITC-labelled anti-CD7 antibody could only bind to

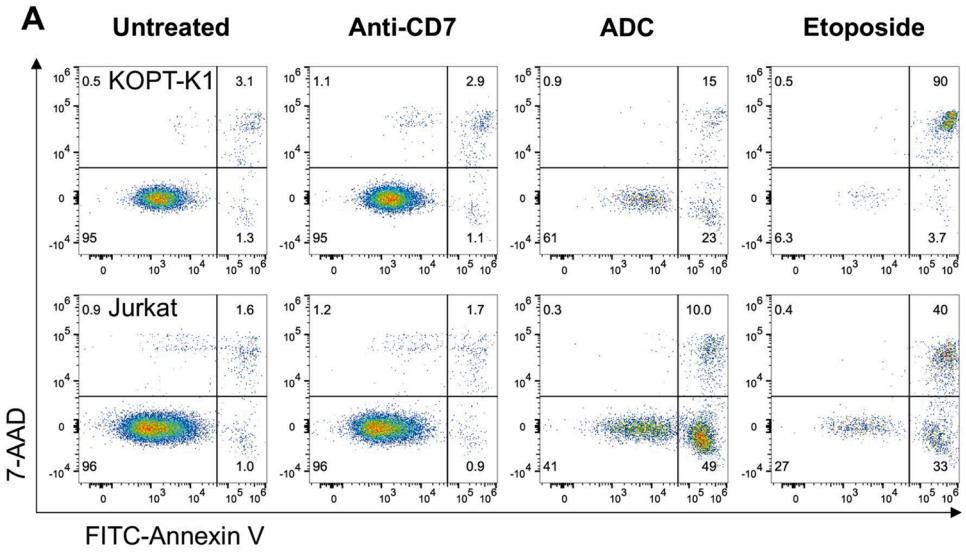

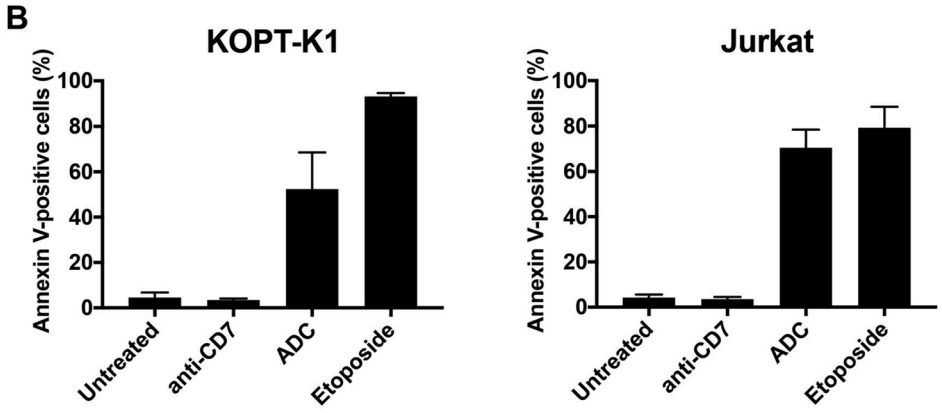

Fig. 3. ADC cytotoxicity occurs by apoptosis induction of CD7-expressing cells.
KOPT-K1 and Jurkat cells were incubated with anti-CD7 antibody or anti-CD7-MMAE ADC (or etoposide as a control) for 24 h. The cells were recovered and incubated with FITC-labelled Annexin V and 7-AAD. The early apoptotic cells are Annexin V-positive, 7AAD-negative and late apoptotic cells are Annexin V-positive, 7AAD-positive (panel A). The columns show the double fluorescence signals for untreated cells, anti-CD7 IgG treated cells and anti-CD7 ADC treated cells. The right-hand panel shows the annexin/7-AAD profiles of cells treated with etoposide for 24 h.
Panel B summarizes data of 3 or more independent experiments and the error bars are standard deviations.

splenocytes from the hCD7 transgenic mice injected with PBS but not with anti-CD7 or anti-CD7 ADC (Fig. 4A).

The fate of the injected ADC was determined by isolating splenocytes from ADC-injected hCD7 mice and carrying out immunofluorescence with anti-EEA1 and anti-LAMP1 (Fig. 4B, C) or anti-human Ig antibody (to detect injected ADC, Figure D, E) and These data show that the ADCs internalize and co-localize with endosome and lysosome markers.

3.5. *Anti-CD7-MMAE ADC activity in cancer-derived xenotransplantation mouse model*

The therapeutic potential of anti-CD7-MMAE was assessed *in vivo* using a cancer cell line derived xenograft model. A549-CD7 cells were implanted sub-cutaneously and when tumours reached a visible size (approximately 100−150 mm^3), the mice were injected with a single dose of anti-CD7 antibody or anti-CD7-MMAE ADC (Fig. 5A) and growth was measured for 36 days. All treatments were generally well tolerated, with no adverse effects on animal appearance or behaviour during the study. The mean bodyweight of all treatment groups increased throughout the study (Supplementary Fig. S4). The tumour growth curves are shown in Fig. 5B. Treatment with anti-CD7 antibody at 2 mg/kg did not result in a significant reduction in tumour growth in comparison with vehicle treated controls ($p = 0.597$ (Table 1)). Treatment with anti-CD7 antibody at 10 mg/kg and treatment with anti-CD7-MMAE at 2 mg/kg and 10 mg/kg resulted in a significant reduction in tumour growth in comparison with vehicle treated controls ($p = 0.016$, $p = 0.013$ and $p = 0.010$ respectively (Table 1)). The increase of ADC dose to 10 mg/kg had a marginal increased effect as the saturation dose is between 2 mg/kg and 10 mg/kg and thus higher doses are unable to deliver more MMAE into the tumour and induce greater cell killing. CD7 antibody at 2 mg/kg had little effect on tumour growth while the ADC at 2 mg/kg shows a substantial inhibitory effect when compared to vehicle. These data show that targeting surface expressed CD7 with ADC, even at a single dose, was effective in inhibiting the growth of sub-cutaneous tumours. The moderate inhibitory effect of dosing antibody at 10 mg/kg was probably due to the athymic nude mice still having NK cells and macrophages present which may induce antibody-dependent cellular toxicity [34].

4. Discussion

CD7 is highly expressed on the cell surface of most, if not all, human T-cell acute lymphoblastic leukaemia cells as well as on the leukaemia initiating cells, making it an attractive therapeutic target for T-ALL. Although CD7 is also expressed on normal T cells and NK cells, it is absent on at least a sub-population of mature T cells [15], which could help in maintaining immune functions after treatment with CD7 targeting agents. In addition, CD7 expression level has been found to be significantly upregulated in T-ALL cells compared to normal CD7-positive T cells [19]. Recent studies also revealed that approximately 30 % of AML cells are CD7-positive, suggesting these AML patients could also benefit from anti-CD7 ADC treatments [21,22]. Several CD7 targeting reagents have been developed over the past decades in various forms including mouse monoclonal antibody [23], single-chain Fv [24], and llama-derived VHH nanobody [25]. While the monoclonal anti-CD7 antibody only showed weak inhibition of tumour growth [23],

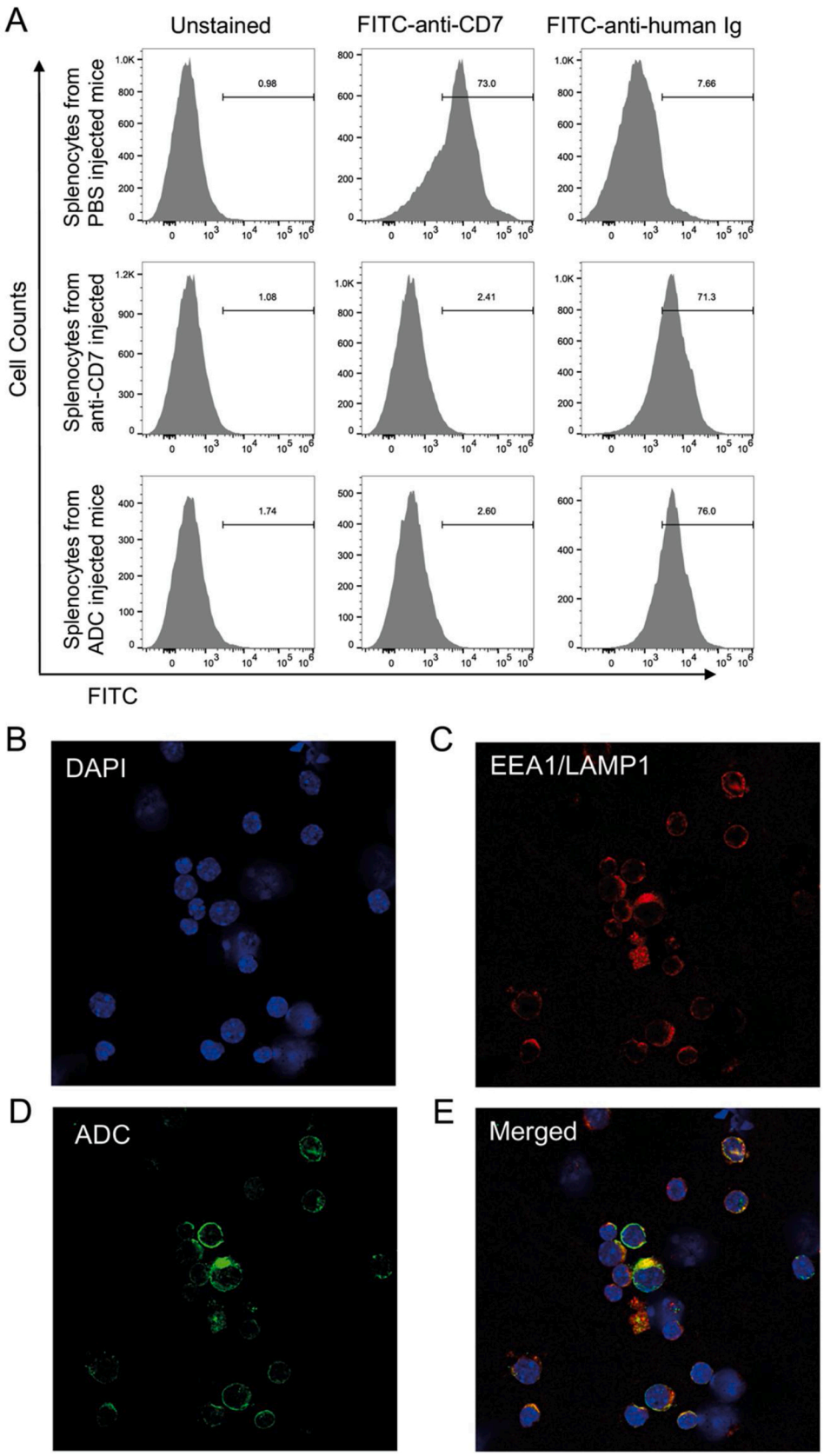

Fig. 4. Localization study of anti-CD7 and anti-CD7 ADC treated transgenic mice expressing human CD7.

Transgenic mice expressing human CD7 [33] were tail vein injected with anti-CD7 IgG, anti-CD7-MMAE ADC or vehicle (PBS) and splenocytes were prepared 4 h after injection. Surface CD7 (panel A) or intracellular anti-CD7 ADC (panel B–E) were examined.

Panel A: splenocytes were stained with FITC-labelled anti-CD7 (middle column) or FITC-labelled anti-human Ig antibody (right hand column).

Panels B-E: The splenocytes of anti-CD7-MMAE ADC injected transgenic mice expressing human CD7 were fixed and incubated with rabbit monoclonal anti-mouse endosomal marker EEA1 or anti-mouse lysosomal marker LAMP1, followed by incubation with Alexa Fluor 594-labeled (red) secondary anti-rabbit antibody (to detect monoclonal antibody bound to EEA1 and LAMP1; panel C) and Alexa Fluor 488-labeled (green) anti-human antibody (to detect the ADCs; panel D). Cell nuclei were stained using DAPI (blue, panel B). The co-localization (yellow) of the ADCs and endosome/lysosome markers is showed in the merged panel E.

A.

Group	n	Treatment Group	Dose	Dosing route	Dosing occasions
1	5	Vehicle	n/a	i.v.	Single dose
2	5	Anti-CD7	2 mg/kg	i.v.	Single dose
3	5	Anti-CD7	10 mg/kg	i.v.	Single dose
4	5	Anti-CD7-MMAE	2 mg/kg	i.v.	Single dose
5	5	Anti-CD7-MMAE	10 mg/kg	i.v.	Single dose

B.

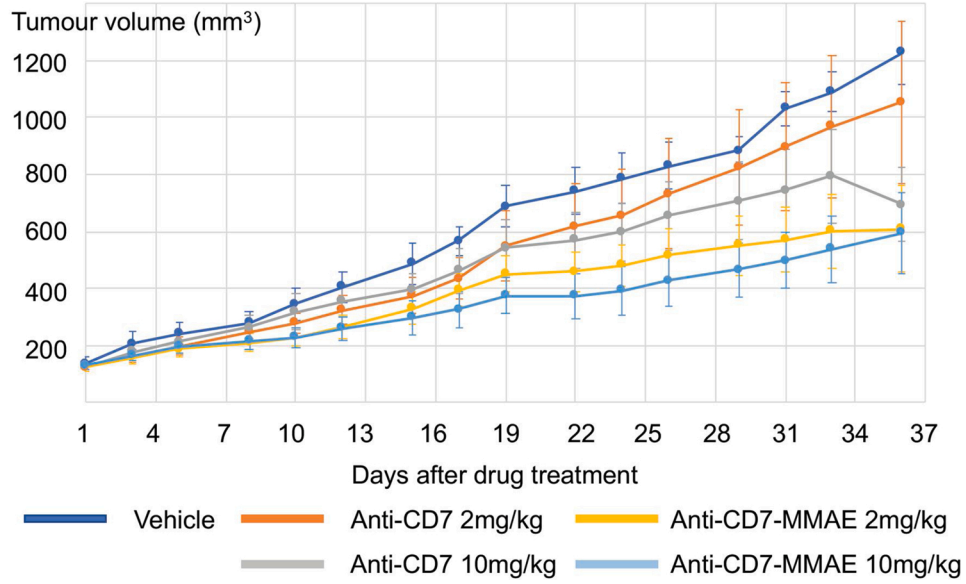

Fig. 5. Anti-CD7-MMAE affects growth of CD7-expressing human cancer cell xenografts. Athymic nude mice were subcutaneously implanted with A549-CD7 cells and randomly assigned to treatment groups when the tumours reached 100–150 mm^3. Animals were intravenously injected with a single dose of PBS (vehicle), anti-CD7 antibody, and anti-CD7-MMAE ADC on day 1 *via* tail vein (A). The tumour growth was measured for 36 days (B) Values shown are mean ± SEM; n = 5 for all groups.

Table 1
Mean starting and final volumes (Day 36) of A549-CD7 tumours implanted subcutaneously in male athymic nude mice dosed with anti-CD7 or anti-CD7-MMAE.

Treatment Group	Treatment	n	Mean Starting Volume mm^3 (SEM)	Mean Final Volume (Day 36) mm^3 (SEM)	p-value compared to vehicle control (Day 36)	T/C Value (%)
1	Vehicle	5	137.6 (20.6)	1227.9 (110.8)	n/a	n/a
2	Anti-CD7 2 mg/Kg	5	125.2 (15.9)	1055.8 (284.7)	0.597 (ns)	85.4
3	Anti-CD7 10 mg/Kg	5	126.3 (15.0)	694.1 (129.5)	0.016 (*)	52.1
4	Anti-CD7-MMAE 2 mg/Kg	5	127.5 (14.4)	607.9 (151.1)	0.013 (*)	44.1
5	Anti-CD7-MMAE 10 mg/Kg	5	129.6 (12.1)	594.6 (142.2)	0.010 (**)	42.6

some immunotoxins-conjugated to anti-CD7 agents demonstrated cell-killing effects on CD7 positive cells but with unacceptable toxicity [26]. ADC technologies promise to greatly improve efficacy and off-target toxicities as they rely on tumour specific delivery of a highly potent toxin. A critical factor for the success of an ADC is the efficient internalization of antigen-ADC complexes to deliver sufficient intracellular concentration of payload to kill target cells [35].

The combination of the monoclonal antibody and the potent cytotoxic drug results in a therapeutic with a highly desirable pharmacodynamic profile if the drug remains stably linked to the antibody until the ADC is processed within the target cell, the specific delivery of anticancer drug minimizes dose-limiting toxicity and maximizes therapeutic effects. Potent cytotoxic molecules such as microtubule destabilizers (MMAE, MMAF, DM1 and DM4) and DNA-damaging drugs (duocarmycin, PBDs and calicheamicin) are too toxic to be used as free drugs. Conjugating these highly potent molecules to antibodies can achieve specific killing of target cancer cells that express the antigen. This approach has resulted in the approval of several ADCs for use in various indications, such as Trastuzumab emtansine (anti-Her2-DM1) [36], Brentuximab vedotin (anti-CD30-MMAE) [28] and Gemtuzumab ozogamicin (anti-CD33-calicheamicin) [37].

Since the CD7 antigen is widely expressed in T cell acute leukaemia and in at least one third of AML, we have employed an anti-CD7 ADC to evaluate the potential of ADCs as an important second stage therapy for T cell acute leukaemia. The anti-CD7-MMAE ADC was designed by linking the potent cytotoxic molecule MMAE with a human IgG1-based chimaeric antibody recognizing CD7 to create the ADC. The linkage of MMAE was made using the highly stable PermaLink® conjugation chemistry [30] which is a cysteine-specific, vinyl pyridine-based chemistry that demonstrates inherent conjugation stability and is not susceptible to drug de-conjugation as it does not undergo the retro-Michael reaction [38]. This allows the potent cytotoxic agent, MMAE, to be safely circulated until the ADC locates CD7-expressing

tumour cells. The anti-CD7-MMAE ADC undergoes rapid internalization once bound to the CD7 antigen on target cells and is trafficked into lysosomes where ADC processing occurs. Cathepsin cleavage of the val-cit moiety followed by self-immolation of the p-aminobenzyl (PAB) spacer releases free toxin leading to cell death by apoptosis.

We have observed that anti-CD7-MMAE ADC displays a potent and selective effect against CD7-expressing cells both *in vitro* and *in vivo*. CD7-expressing T cell lines, such as Jurkat and KOPT-K1, are sensitive to the ADC with an IC_{50} of less than 10 nanogram per milliliter (8.1 ng/mL and 5.4 ng/mL respectively). The growth of CD7-negative cells was not affected by ADC at microgram per milliliter levels. The efficacy of the anti-CD7 ADC, compared to mice treated with antibody alone, was assessed in immunodeficient mice implanted with the CD7 transfected A549 (A549-CD7) cell line. The anti-CD7 antibody is specific to the human antigen expressed in the xenograft and does not cross react with mouse CD7. The treatments were generally well tolerated as decreases in body weight (used as an indirect measure of toxicity) were not observed during the study. Treatment with anti-CD7 alone at 2 mg/kg did not result in a significant reduction in tumour growth in comparison with vehicle treated controls. Mice received single doses of ADC (either 2 mg/kg or 10 mg/kg) and both resulted in a significant reduction in tumour growth in comparison with the vehicle treated control group. However, tumour regression was not observed even at the dose of 10 mg/kg and there was only a marginal decrease in tumour growth when the dose was increased from 2 mg/kg to 10 mg/kg, suggesting that the saturation dose in the A549-CD7 CDX model had been reached. By increasing the DAR of future ADCs, an improvement in *in vivo* efficacy could be achieved by allowing more payload per antibody to be delivered to the tumour at the saturation dose. In addition, utilising more potent payloads with alternative modes of action, such as pyrrolobenzodiazepine, could lead to an improvement in efficacy and expand the scope of anti-CD7 ADCs. There was also some effect of the anti-CD7 antibody alone at 10 mg/kg (p value 0.016) as this dose also slows growth but less substantially than the ADC (p value 0.010). The recipient mice for this study were homozygous nude mice that retain NK cells and macrophages. These innate immunity cells are probably responsible for the non-ADC induced tumour inhibition effect *via* antibody-dependent cell-mediated cytotoxicity.

While several ADCs have been developed and have achieved various levels of success in treating leukaemia, few of them focused on T-ALL. We expect that ADCs could prove to be important therapeutic options for treating T-ALL, and all CD7-expressing leukaemias including the relevant AMLs. In particular, this has great potential for relapsed, refractory disease in which patients have few further treatment options. There is no significant CD7 expression on most hematopoietic progenitor cells (16). Therefore, an immunotoxin directed against CD7 has a promising range of prospective applications against T-cell neoplasms. Although a greater fraction of T-cell leukaemias and some cases of AML express CD7 on their surface, the CD7 ADC would still avoid eliminating all normal T cells important for the maintenance of relevant immune functions, because it would spare the CD7-negative subset of normal T-lymphoid cells (23). Finally, future ADC designs could incorporate antibodies binding to TCR receptor constant regions. There are two human TCRB constant regions (Cβ1 and Cβ2) [39] and an antibody that binds only to Cβ1 that has been incorporated into CAR-T cells [40]. A bispecific anti-CD7/anti- Cβ1 antibody would have the added advantage of only targeting those T cells expressing Cβ1 (tumours and normal T cells) and not those expressing Cβ2. This would leave a functional T cell population after therapy which would be hugely beneficial for older T-ALL patients.

Author's contributions

Originators of project: THR
Participated in research design: JZ, AJ, SM, DW, JM, JT, AM, THR
Conducted experiments: JZ, AJ, SM, DW, AL, MAN, AM
Performed data analysis: JZ, AJ, SM, DW, JM, AL, JT, AM, THR,
Wrote or contributed to the writing of the manuscript: all authors

Additional information

Supplementary Information accompanies this paper

Declaration of Competing Interest

The authors have no conflicts of interest to declare.

Acknowledgements

This work was supported by grants from Blood Cancer IUK12051 and EPSRCEP/L024012/1. We wish to thank Dr. Georg Fey for the pET26b anti-CD7 scFv cys vector and Dr. Linda Baum for the pcDNA3.1-ZEO CD7 vector. We also thank Dr Marc Mansour for the KOPTI-KI cells and Dr. Chris Birchall for useful discussions on this work.

Appendix A. Supplementary data

Supplementary material related to this article can be found, in the online version, at doi:https://doi.org/10.1016/j.leukres.2021.106626.

References

[1] G.M. Dores, S.S. Devesa, R.E. Curtis, M.S. Linet, L.M. Morton, Acute leukemia incidence and patient survival among children and adults in the United States, 2001-2007, Blood 119 (1) (2012) 34–43.
[2] S.P. Hunger, C.G. Mullighan, Acute lymphoblastic leukemia in children, N. Engl. J. Med. 373 (16) (2015) 1541–1552.
[3] A.K. Fielding, S.M. Richards, R. Chopra, H.M. Lazarus, M.R. Litzow, G. Buck, I. J. Durrant, S.M. Luger, D.I. Marks, I.M. Franklin, A.K. McMillan, M.S. Tallman, J. M. Rowe, A.H. Goldstone, A.L.L.W.P. Medical Research Council of the United Kingdom Adult, G. Eastern Cooperative Oncology, Outcome of 609 adults after relapse of acute lymphoblastic leukemia (ALL); an MRC UKALL12/ECOG 2993 study, Blood 109 (3) (2007) 944–950.
[4] K. Karrman, B. Johansson, Pediatric T-cell acute lymphoblastic leukemia, Genes Chromosomes Cancer 56 (2) (2017) 89–116.
[5] E.H. Phillips, S. Devereux, J. Radford, N. Mir, T. Adedayo, L. Clifton-Hadley, R. Johnson, Toxicity and efficacy of alemtuzumab combined with CHOP for aggressive T-cell lymphoma: a phase 1 dose-escalation trial, Leuk. Lymphoma 60 (9) (2019) 2291–2294.
[6] T. Boehm, L. Foroni, Y. Kaneko, M.F. Perutz, T.H. Rabbitts, The rhombotin family of cysteine-rich LIM-domain oncogenes: distinct members are involved in T-cell translocations to human chromosomes 11p15 and 11p13, Proc. Natl. Acad. Sci. U. S. A. 88 (10) (1991) 4367–4371.
[7] I.D. Dube, S. Kamel-Reid, C.C. Yuan, M. Lu, X. Wu, G. Corpus, S.C. Raimondi, W. M. Crist, A.J. Carroll, J. Minowada, et al., A novel human homeobox gene lies at the chromosome 10 breakpoint in lymphoid neoplasias with chromosomal translocation t(10;14), Blood 78 (11) (1991) 2996–3003.
[8] L.R. Finger, J. Kagan, G. Christopher, J. Kurtzberg, M.S. Hershfield, P.C. Nowell, C. M. Croce, Involvement of the TCL5 gene on human chromosome 1 in T-cell leukemia and melanoma, Proc. Natl. Acad. Sci. U. S. A. 86 (13) (1989) 5039–5043.
[9] E.A. McGuire, R.D. Hockett, K.M. Pollock, M.F. Bartholdi, S.J. O'Brien, S. J. Korsmeyer, The t(11;14)(p15;q11) in a T-cell acute lymphoblastic leukemia cell line activates multiple transcripts, including Ttg-1, a gene encoding a potential zinc finger protein, Mol. Cell. Biol. 9 (5) (1989) 2124–2132.
[10] J.D. Mellentin, S.D. Smith, M.L. Cleary, lyl-1, a novel gene altered by chromosomal translocation in T cell leukemia, codes for a protein with a helix-loop-helix DNA binding motif, Cell 58 (1) (1989) 77–83.
[11] B. Royer-Pokora, U. Loos, W.D. Ludwig, TTG-2, a new gene encoding a cysteine-rich protein with the LIM motif, is overexpressed in acute T-cell leukaemia with the t(11;14)(p13;q11), Oncogene 6 (10) (1991) 1887–1893.
[12] J. Wang, S.N. Jani-Sait, E.A. Escalon, A.J. Carroll, P.J. de Jong, I.R. Kirsch, P. D. Aplan, The t(14;21)(q11.2;q22) chromosomal translocation associated with T-cell acute lymphoblastic leukemia activates the BHLHB1 gene, Proc. Natl. Acad. Sci. U. S. A. 97 (7) (2000) 3497–3502.
[13] Y. Xia, L. Brown, C.Y. Yang, J.T. Tsan, M.J. Siciliano, R. Espinosa 3rd, M.M. Le Beau, R.J. Baer, TAL2, a helix-loop-helix gene activated by the (7;9)(q34;q32) translocation in human T-cell leukemia, Proc. Natl. Acad. Sci. U. S. A. 88 (24) (1991) 11416–11420.
[14] R.C. Larson, H. Osada, T.A. Larson, I. Lavenir, T.H. Rabbitts, The oncogenic LIM protein Rbtn2 causes thymic developmental aberrations that precede malignancy in transgenic mice, Oncogene 11 (5) (1995) 853–862.
[15] U. Reinhold, L. Liu, J. Sesterhenn, H. Abken, CD7-negative T cells represent a separate differentiation pathway in a subset of post-thymic helper T cells, Immunology 89 (3) (1996) 391–396.

[16] A.S. Chan, J.L. Mobley, G.B. Fields, Y. Shimizu, CD7-mediated regulation of integrin adhesiveness on human T cells involves tyrosine phosphorylation-dependent activation of phosphatidylinositol 3-kinase, J. Immunol. 159 (2) (1997) 934–942.
[17] R. Stillwell, B.E. Bierer, T cell signal transduction and the role of CD7 in costimulation, Immunol. Res. 24 (1) (2001) 31–52.
[18] S.G. Ward, R. Parry, C. LeFeuvre, D.M. Sansom, J. Westwick, A.I. Lazarovits, Antibody ligation of CD7 leads to association with phosphoinositide 3-kinase and phosphatidylinositol 3,4,5-trisphosphate formation in T lymphocytes, Eur. J. Immunol. 25 (2) (1995) 502–507.
[19] H. Pais, K. Ruggero, J. Zhang, O. Al-Assar, N. Bery, R. Bhuller, V. Weston, P. R. Kearns, C. Mecucci, A. Miller, T.H. Rabbitts, Surfaceome interrogation using an RNA-seq approach highlights leukemia initiating cell biomarkers in an LMO2 T cell transgenic model, Sci. Rep. 9 (1) (2019) 5760.
[20] B. Gerby, E. Clappier, F. Armstrong, C. Deswarte, J. Calvo, S. Poglio, J. Soulier, N. Boissel, T. Leblanc, A. Baruchel, J. Landman-Parker, P.H. Romeo, P. Ballerini, F. Pflumio, Expression of CD34 and CD7 on human T-cell acute lymphoblastic leukemia discriminates functionally heterogeneous cell populations, Leukemia 25 (8) (2011) 1249–1258.
[21] H. Chang, F. Salma, Q.L. Yi, B. Patterson, B. Brien, M.D. Minden, Prognostic relevance of immunophenotyping in 379 patients with acute myeloid leukemia, Leuk. Res. 28 (1) (2004) 43–48.
[22] G. Del Poeta, R. Stasi, A. Venditti, C. Cox, G. Aronica, M. Masi, A. Bruno, M. D. Simone, F. Buccisano, G. Papa, CD7 expression in acute myeloid leukemia, Leuk. Lymphoma 17 (1–2) (1995) 111–119.
[23] W. Baum, H. Steininger, H.J. Bair, W. Becker, T.E. Hansen-Hagge, M. Kressel, E. Kremmer, J.R. Kalden, M. Gramatzki, Therapy with CD7 monoclonal antibody TH-69 is highly effective for xenografted human T-cell ALL, Br. J. Haematol. 95 (2) (1996) 327–338.
[24] M. Peipp, H. Kupers, D. Saul, B. Schlierf, J. Greil, S.J. Zunino, M. Gramatzki, G. H. Fey, A recombinant CD7-specific single-chain immunotoxin is a potent inducer of apoptosis in acute leukemic T cells, Cancer Res. 62 (10) (2002) 2848–2855.
[25] J. Tang, J. Li, X. Zhu, Y. Yu, D. Chen, L. Yuan, Z. Gu, X. Zhang, L. Qi, Z. Gong, P. Jiang, J. Yu, H. Meng, G. An, H. Zheng, L. Yang, Novel CD7-specific nanobody-based immunotoxins potently enhanced apoptosis of CD7-positive malignant cells, Oncotarget 7 (23) (2016) 34070–34083.
[26] A.E. Frankel, J.H. Laver, M.C. Willingham, L.J. Burns, J.H. Kersey, D.A. Vallera, Therapy of patients with T-cell lymphomas and leukemias using an anti-CD7 monoclonal antibody-ricin A chain immunotoxin, Leuk. Lymphoma 26 (3–4) (1997) 287–298.
[27] A.M. Soler-Rodriguez, M.A. Ghetie, N. Oppenheimer-Marks, J.W. Uhr, E.S. Vitetta, Ricin A-chain and ricin A-chain immunotoxins rapidly damage human endothelial cells: implications for vascular leak syndrome, Exp. Cell Res. 206 (2) (1993) 227–234.
[28] J.A. Francisco, C.G. Cerveny, D.L. Meyer, B.J. Mixan, K. Klussman, D.F. Chace, S. X. Rejniak, K.A. Gordon, R. DeBlanc, B.E. Toki, C.L. Law, S.O. Doronina, C. B. Siegall, P.D. Senter, A.F. Wahl, cAC10-vcMMAE, an anti-CD30-monomethyl auristatin E conjugate with potent and selective antitumor activity, Blood 102 (4) (2003) 1458–1465.
[29] C. Li, C. Zhang, Z. Li, D. Samineni, D. Lu, B. Wang, S.C. Chen, R. Zhang, P. Agarwal, B.M. Fine, S. Girish, Clinical pharmacology of vc-MMAE antibody-drug conjugates in cancer patients: learning from eight first-in-human Phase 1 studies, MAbs 12 (1) (2020), 1699768.
[30] Iksuda, Patents, EP2373675, EP2886132, US8785595, and US9212148.
[31] L. Persic, A. Roberts, J. Wilton, A. Cattaneo, A. Bradbury, H.R. Hoogenboom, An integrated vector system for the eukaryotic expression of antibodies or their fragments after selection from phage display libraries, Gene 187 (1) (1997) 9–18.
[32] H.D. King, G.M. Dubowchik, H. Mastalerz, D. Willner, S.J. Hofstead, R.A. Firestone, S.J. Lasch, P.A. Trail, Monoclonal antibody conjugates of doxorubicin prepared with branched peptide linkers: inhibition of aggregation by methoxytriethyleneglycol chains, J. Med. Chem. 45 (19) (2002) 4336–4343.
[33] L.E. Schanberg, D.M. Lee, D.E. Fleenor, R.E. Ware, D.D. Patel, B.F. Haynes, R. E. Kaufman, Characterization of human CD7 transgenic mice, J. Immunol. 155 (5) (1995) 2407–2418.
[34] M. Barok, J. Isola, Z. Palyi-Krekk, P. Nagy, I. Juhasz, G. Vereb, P. Kauraniemi, A. Kapanen, M. Tanner, G. Vereb, J. Szollosi, Trastuzumab causes antibody-dependent cellular cytotoxicity-mediated growth inhibition of submacroscopic JIMT-1 breast cancer xenografts despite intrinsic drug resistance, Mol. Cancer Ther. 6 (7) (2007) 2065–2072.
[35] C.H. Chau, P.S. Steeg, W.D. Figg, Antibody-drug conjugates for cancer, Lancet 394 (10200) (2019) 793–804.
[36] W.C. Widdison, S.D. Wilhelm, E.E. Cavanagh, K.R. Whiteman, B.A. Leece, Y. Kovtun, V.S. Goldmacher, H. Xie, R.M. Steeves, R.J. Lutz, R. Zhao, L. Wang, W. A. Blattler, R.V. Chari, Semisynthetic maytansine analogues for the targeted treatment of cancer, J. Med. Chem. 49 (14) (2006) 4392–4408.
[37] P.R. Hamann, L.M. Hinman, I. Hollander, C.F. Beyer, D. Lindh, R. Holcomb, W. Hallett, H.R. Tsou, J. Upeslacis, D. Shochat, A. Mountain, D.A. Flowers, I. Bernstein, Gemtuzumab ozogamicin, a potent and selective anti-CD33 antibody-calicheamicin conjugate for treatment of acute myeloid leukemia, Bioconjug. Chem. 13 (1) (2002) 47–58.
[38] M. Frigerio, A.F. Kyle, The chemical design and synthesis of linkers used in antibody drug conjugates, Curr. Top. Med. Chem. 17 (32) (2017) 3393–3424.
[39] J.E. Sims, A. Tunnacliffe, W.J. Smith, T.H. Rabbitts, Complexity of human T-cell antigen receptor beta-chain constant- and variable-region genes, Nature 312 (5994) (1984) 541–545.
[40] P.M. Maciocia, P.A. Wawrzyniecka, B. Philip, I. Ricciardelli, A.U. Akarca, S. C. Onuoha, M. Legut, D.K. Cole, A.K. Sewell, G. Gritti, J. Somja, M.A. Piris, K. S. Peggs, D.C. Linch, T. Marafioti, M.A. Pule, Targeting the T cell receptor beta-chain constant region for immunotherapy of T cell malignancies, Nat. Med. 23 (12) (2017) 1416–1423.